Spatio-temporal Spectral Variability in Cassiopeia A

Yamini Nambiar[1], Vinay Kashyap[2], and Dan Patnaude[2]

[1]Acton-Boxborough Regional High School, Acton, MA

[2]Harvard Smithsonian Center for Astrophysics, Cambridge, MA

Summary

We have analyzed the supernova remnant, Cassiopeia A (see Fig. 1), and have identified regions with large spectral abnormalities and variability over the past decade. Cas A is known to be the strongest radio source in the sky beyond our solar system with an estimated explosion date of around AD 1670 (Thorstensen et al. 2001; see also Table 1). Here, we flagged pixels that showed large departures from renormalized color light curves. We combined these pixels at various spatial scales to create maps of interesting regions that show spectral variability in the remnant during the Chandra mission (Fig. 3). In addition, we identify intrinsic spectral abnormalities in Cas A by flagging atypical hardness ratios at each epoch (Fig. 4). We show that many sites of this spectral irregularity exist and that these sites coincide with prominent features on the remnant. Specifically, we found that features at the edge of the remnant, the central compact object, and numerous knots within Cas A correspond to our identified regions (see Results). A sample of the detected pixels is shown in Table 2 and Table 3. The full list of pixel locations is accessible from the Harvard Dataverse Network, at http://dx.doi.org/10.7910/DVN1/22634.

Analysis

We limit our analysis to those pixels which pass the following criteria: at least 200 counts, at least 1 count in each observation in each passband, and at least 5e-6 ct/s/pix (at a binning of 4) to exclude background pixels. We detect interesting regions on Cas A based on a statistical analysis of spectra and color light curves. This strategy is similar to the spatial image segmentation employed by Sanders (2006; however we apply thresholds to color light curves) and the spatial grid-based spectral analysis of Yang et al. (2008) and Hwang & Laming (2012), though we consider hardness ratios over time and at different spatial scales.

Regions with Abnormal Intrinsic Hardness Ratios at Each Epoch

For all pixels, we compute light curves in different CSC passbands (soft, medium, and hard). These light curves are then used to generate color light curves (log_{10}(soft/medium) and log_{10} (medium/hard)). We then flag those areas of the remnant which show an abnormal spectral signature. We compute the mean of the colors at each epoch and find all pixels which show deviations of >3σ from the mean. Based on these pixels, we map out the regions on Cas A that show locations that exhibit abnormal intrinsic hardness ratios. These regions are shown in Figure 3 and listed in Table 2.

Regions with Spectral Variability

For all pixels, color light curves are also generated. These curves are then renormalized by their mean and flagged for large variability. We compute the standard deviation of the light curves across the epochs for each pixel. We then flag those pixels where the standard deviation is large, determined as >3σ from the mean of the standard deviation, as locations that show large variability. These pixels are shown in Figure 4 and are listed in Table 3.

Dataverse Network

Scan the QR code to access full region lists on the Harvard Dataverse Network.

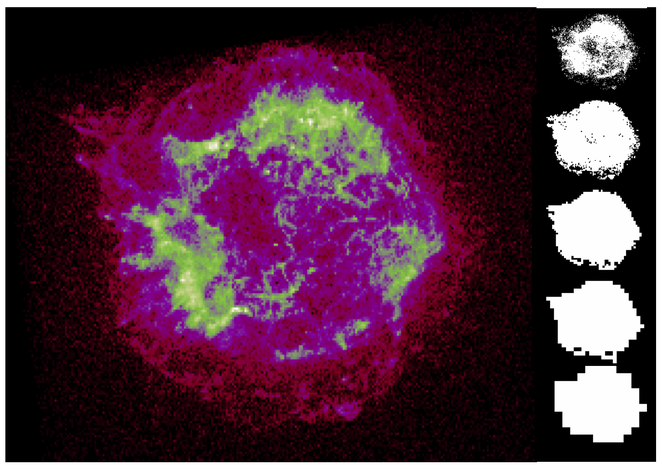

Fig. 1 ACIS image of Cas A. Scaling in bin 1. The 5 bitmap images to the right show ObsID 198 of masks in the passband bins 4, 8, 16, 32, and 64 from top to bottom. White areas are regions where pixel values were included in spatial and temporal variability calculations. All masks pass criteria listed in the Analysis section.

Table 1:
Physical Parameters for Cas A

RA , DEC	23:23:24 +58:48.9	SIMBAD
(l_{II}, b_{II})	(111.735, -02.130)	SIMBAD
Age	~330 years	Thorstensen et al. 2001
Distance	3.4 kpc	Koralesky et al. 2008
Angular Size	5x5 arcmin	Koralesky et al. 2008

Table 2 (incomplete):
Regions with Abnormal Intrinsic Hardness Ratios at Each Epoch

RA	DEC	Ratio	Bin	Quality*
23:23:30.114	+58:51:17.58	soft/medium	4	1.40065
23:23:27.196	+58:51:30.37	soft/medium	8	1.02270
23:23:25.928	+58:51:24.47	medium/hard	16	1.12596
23:23:10.224	+58:48:27.28	medium/hard	32	1.04635
23:23:13.265	+58:48:19.43	soft/medium	64	1.17623

Table 3 (incomplete):
Regions with Spectral Variability Over Epochs

RA	DEC	Ratio	Bin	Quality*
23:23:25.040	+58:51:17.58	soft/medium	4	5.88427
23:23:18.572	+58:51:14.61	soft/medium	8	6.14943
23:23:49.239	+58:48:46.91	medium/hard	16	7.07846
23:23:36.565	+58:47:24.35	soft/medium	32	6.26237
23:23:17.308	+58:50:25.40	medium/hard	64	5.20881
23:23:37.595	+58:50:56.89	medium/hard	64	5.54720

*Quality is a measure of the ratio of the selection criteria to the threshold. The higher the quality number the higher the significance.

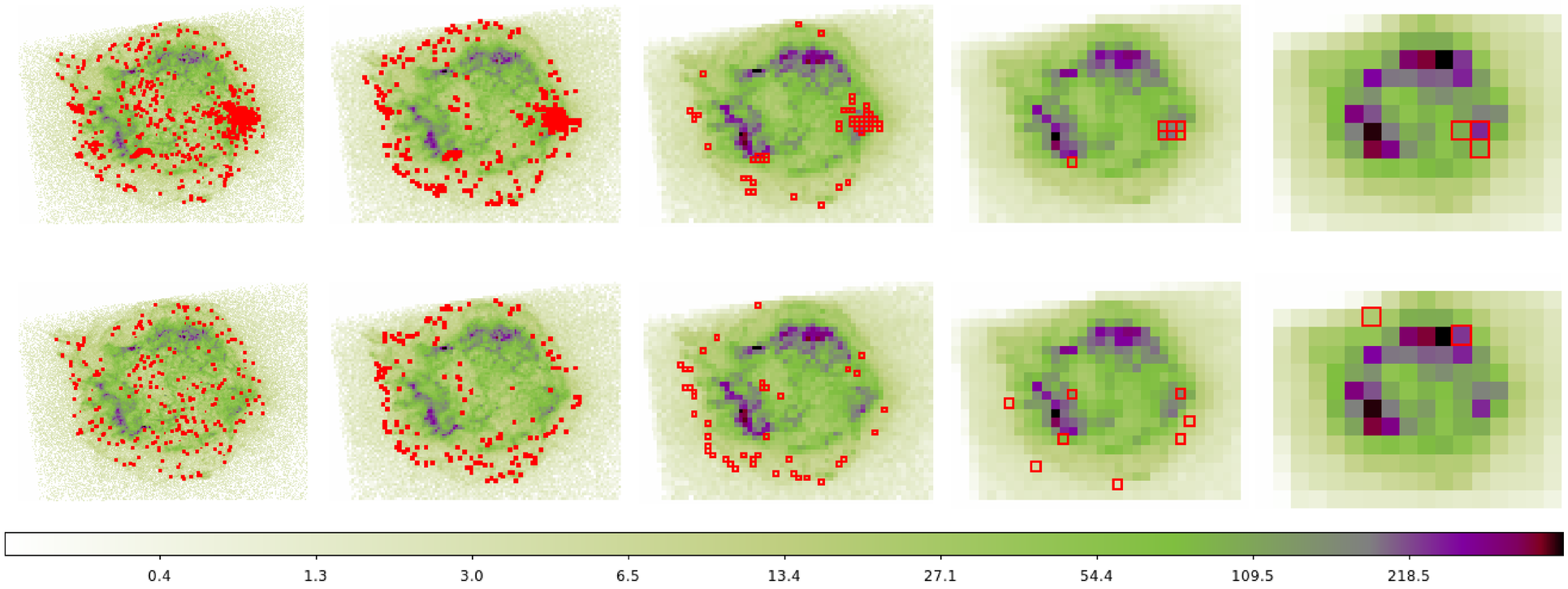

Fig. 3 Spectrally abnormal regions (red boxes) found at different binnings, overlaid on corresponding Cas A images. Regions found using both colors are displayed. The underlying image is the log-scaled counts from ObsID 198 in the 0.3-8 keV band. The color bar corresponds to the bin=4 case. Top: Regions marked show abnormal intrinsic hardness ratios.

Fig. 4 Bottom: As in Figure 3, but for regions that show large temporal variability.

Results

Hwang, Holt, & Petre, 2000	Compared X-ray emission-line maps in ejecta of Si, S, Ar, Ca, and Fe abundance with continuum emission.	Locations of abnormal spectral sites found at binsize=64 (Fig. 3) coincide with locations of S and Si concentrations. Regions around the central ring of the Si and S ejecta are found but the edges of Fe L, Fe K, and Ca maps are not. The northern Ar region coincides with regions flagged as temporally variable at large binsizes.
Hwang et al. 2004	Identified regions dominated by Si He alpha (1.78-2 keV), Fe K (6.52-6.95 keV), and continuum emission.	The inner part of the jet structure seen in Si is flagged as spectrally abnormal and is time variable. The region identified as the counter-jet is also seen to be spectrally abnormal but temporal variability is offset to larger off-axis locations. The continuum dominated edges are strong sites of both spectral and temporal variability.
Delaney et al. 2004	Separated spatial and kinematic components through high-resolution for Si-, Fe-, low-energy-, and continuum-dominated spectral components.	We find abnormal spectral regions on the West side of Cas A that match continuum dominated regions. None of the regions we find coincide with the locations of the Si- and Fe-dominated structures found by Delaney et al.
Patnaude & Fesen 2007	Detected several small-scale structures that exhibit significant intensity and temperature changes at various locations around the remnant.	Regions R3 and R4 are picked up in our analysis as time variable with R2 and R6 as spectrally abnormal. R1 and R5 are flagged as spectro-temporally variable at smaller binsizes (Fig. 3 & Fig. 4).
Uchiyama & Aharonian 2008	Found year-scale time variations in X-ray intensity for multiple X-ray filaments and knots.	All areas of variable X-ray filaments coincide with temporal spectral variation (Fig. 4).
Yang ,Chen , & Li 2008	As in Hwang & Laming (2012), carried out spectral analysis on a grid covering Cas A to produce maps of absorption column, ionization age, redshift, temperature, and abundances of Si, Ca, and Fe.	The temperature, absorption column, and redshift maps do not show a correlation with sites of spectral abnormality or spectro-temporal variability. On the other hand, the site at West of center that we find to be variable does have large values of these parameters. Regions with large spectral variability overlap those with large Si, Ca, and Fe abundance in the jet and in the West-central region.
Patnaude & Fesen 2009	Identified various filaments around the edge of the remnant which show changes in X-ray intensity.	All of the regions are detected in our analysis as spectro-temporally variable. We find a large number of pixels around the edge of the remnant at small binsizes that are of interest.
Patnaude at el. 2011	Carried out spectral analysis of multiple regions of size ≈1” around the edge of Cas A and in the interior and found them to vary.	All the regions around the edge of the remnant are found to be spectro-temporally variable. The region at West of center is found to be strongly variable at all scales. However, filaments below the location of the neutron star are not strong sites of spectral or temporal variability.
Hwang & Laming 2012	As in Yang et al. (2008), made comprehensive maps of spectral fit parameters (absorption column, temperature, ionization age, and abundances of Si, Fe, Ne, Mg, S, Ar) at small scales ($\lesssim$ 0.1”). Many regions of elevated values are found around the remnant	Regions with high Si and Fe abundances are correlated with those found to show spectral variability. Regions with high Mg and Ne abundance are flagged as spectrally abnormal and temporally variable.

References

DeLaney, T., Rudnick, L., Fesen, R. A., Jones, T. W., Petre, R., & Morse, J. A. 2004, ApJ, 613, 343
Fruscione et al. 2006, SPIE Proc. 6270, 62701V, D.R. Silvia & R.E. Doxsey, eds.
Koralesky, B., et al., 1998, ApJ, 505, L27
Hwang, U., et al. 2004, ApJ, 615, L117
Hwang, U., Holt, S. S., & Petre, R. 2000, ApJ, 537, L119
Hwang, U., & Laming, J.M. 2012, ApJ, 746, 130
Patnaude, D. J., & Fesen, R. A. 2007, AJ, 133, 147
Patnaude, D. J., & Fesen, R. A. 2009, ApJ, 697, 535
Patnaude, D. J., Vink, J., Laming, J.M., & Fesen, R. A. 2011, AJ, 729, L28
Sanders, J. 2006, Mon.Not.Roy.Astron.Soc., 829, 842
Thorstensen J.R., Fesen R.A., van den Bergh S., 2001, AJ, 122, 297
Uchiyama, Y., & Aharonian, F. A. 2008, ApJ, 677, L105
Yang, X.-J.,Liu, F. J-., & Chen, L. 2008 Chin. J. Astron. Astrophys. 8, 439

Data

We used 8 ACIS-S observations of Cas A (Table 1) spanning the years 2000 to 2012 (Fig. 2). We computed spectral hardness ratios based on the soft, medium, and hard CSC bands over spatial scales that correspond to binning ACIS image pixels by 4, 8, 16, 32, and 64. Across all epochs, a given pixel at a given binning covers the same sky coordinates. As the first step of our procedure, we reduced the data and applied the latest calibration using the CIAO tool chandra_repro. To account for exposure variations, we used exposure maps and computed photon fluxes with the CIAO tool fluximage.

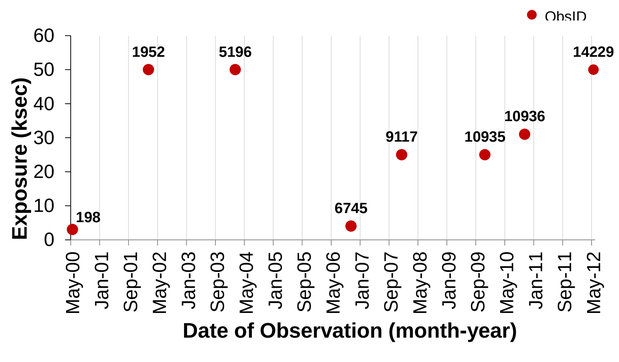

Fig. 2 Exposure times (in ksec) of the observations used here. The ObsIDs, in chronological order, are 198, 1952, 5196, 6745, 9117, 10935, 10936, and 14229.

Acknowledgments

YN thanks Acton-Boxborough Regional High School,Young Einstein’s Science Club, and Suresh Damodaran for support and guidance. VK and DP acknowledge support during this project from the Chandra X-Ray Center.